Iranian Journal of Pharmaceutical Sciences
Spring 2008: 4(2): 157-162
www.ijps.ir

Original Article

Effect of Surfactant in Formation of Hydroxyapatite Nano-Rods under Hydrothermal Conditions

Mehrnaz Salarian[a,*], Mehran Solati-Hashjin[b], Azadeh Goudarzi[b], Seyedeh Sara Shafiei[b], Reza Salarian[c], Ziarat Ali Nemati[a,d],

[a]*School of Materials Engineering, Tehran Science and Research Branch, Islamic Azad University, Tehran, Iran*
[b]*Biomedical Engineering Faculty, Amirkabir University of Technology, Tehran, Iran*
[c]*Maziyar University, School of Engineering, Mazandaran, Noor, Iran*
[d]*Department of Materials Science and Engineering, Sharif University of Technology, Tehran, Iran*

Abstract

Hydroxyapatite (HA) nano-rods with uniform morphology and controllable size have been successfully synthesized in the presence of cationic and non-ionic surfactants by a hydrothermal method. $(NH_4)_2HPO_4$ and $Ca(NO_3)_2.4H_2O$ were used as the phosphorus and calcium sources, respectively. The composition of synthesized powders was characterized using X-ray diffraction, and Fourier transform infrared spectrometer and morphology of the resulting powders were examined by scanning electron microscopy. Results revealed the as-prepared HA nano-rods have a typical diameter of about 60-80 nm and an average aspect ratio of about 10-12, which indicates that the mixture of cationic and non-ionic surfactants acts as a soft template to regulate the nucleation and crystal growth of HA. Also effect of hydrothermal temperature was studied on the system.

Keywords: Hydrothermal; Hydroxyapatite; Nano-rods; Synthesis.
Received: December 10, 2007; *Accepted:* March 5, 2008

Introduction

Hydroxyapatite ($Ca_{10}(PO_4)_6(OH)_2$; HA) nanoparticles have been of great interest because of their mineral components being similar to human hard tissues [1-3]. Synthetic HA has excellent biocompatibility and bioactivity, so it is used in reconstruction of damaged bone or tooth zones [4, 5]. The principal limitation in its clinical use as a load bearing implant is mechanical brittleness. Generally, the fracture strength and fracture toughness of ceramic materials are effectively improved by dispersing rod-like crystals and whiskers into the bulk materials. Thus, rod-like crystals and whiskers of HA sound to be useful as materials for improving the mechanical properties of synthetic biomaterials, etc. [6].

It is well-known that the strength of ceramic fibers and whiskers is of size-dependence. As the diameter or length decreases, the strength of ceramic fibers and whiskers increases. Moreover, their physical properties such as fracture toughness and fracture strength, etc. depend on the crystal structure, composition

*Corresponding author: Mehrnaz Salarian, School of Materials Engineerin, Tehran Science and Research Branch, Islamic Azad University (IAU), Tehran, Iran.
Tel (+98)21-77829564, Fax (+98)21-77829564
E-mail: mehrnazsalarian@gmail.com

and sizes [7].

HA can be synthesized by many chemical-processing routes including solid-state reaction [8], co-precipitation, sol-gel synthesis, pyrolysis of aerosols, microemulsion and hydrothermal reaction [5, 9]. These methods, however, mostly prepare irregular forms of powder [5]. The most attractive method to synthesis nano-rods of HA is using surfactants [1, 10].

In this study, HA nano-rods with uniform morphologies and controllable size have been successfully synthesized in the presence of cetyltrimethylammonium bromide (CTAB) as a cationic surfactant and polyethylene glycol as a non-ionic surfactant. Also influences of hydrothermal temperature on the morphology and size of hydroxyapatite nanoparticles have been investigated.

2. Material and methods

2.1. Materials

The starting materials used in this study were calcium nitrate tetrahydrate ($Ca(NO_3)_2.4H_2O$) (Merck Prolabo 22 384.298), diammonium hydrogen phosphate ($(NH_4)_2HPO_4$) (Merck Prolabo 21 306.293), cetyltrimethylammonium bromide (CTAB) (102342 Merck) and polyethylene glycol (PEG400) (807485 Merck). All chemicals were analytical grade. The Ca/P molar ratio was equal to 1.67 (stoichiometric ratio of HA).

2.2. Methods

The general procedure was the following: 0.03 mole of $(NH_4)_2HPO_4$ and 0.021 mole of CTAB were dissolved completely in 125 ml of deionized water. This solution was stirred with a magnetic stirrer for 30 min to ensure that the cooperative interaction and self-assembly process were completed. Then the pH value was adjusted to 4.5 by adding pure acetic acid. After that, 0.05 mole of $Ca(NO_3)_2.4H_2O$ was dissolved in 175 ml of deionized water and proper amount of PEG400 was simultaneously added to the solution under constant stirring for 30 min. Then the mixed solution of $Ca(NO_3)_2.4H_2O$ and PEG400 was added to the latter dropwise under continuous magnetic stirring in air. The final milky suspension was transferred to an autoclave, sealed tightly and hydrothermally treated in an oven at different temperatures of 90,120 and 150 °C for 22 h. The resultant precipitates were separated from the

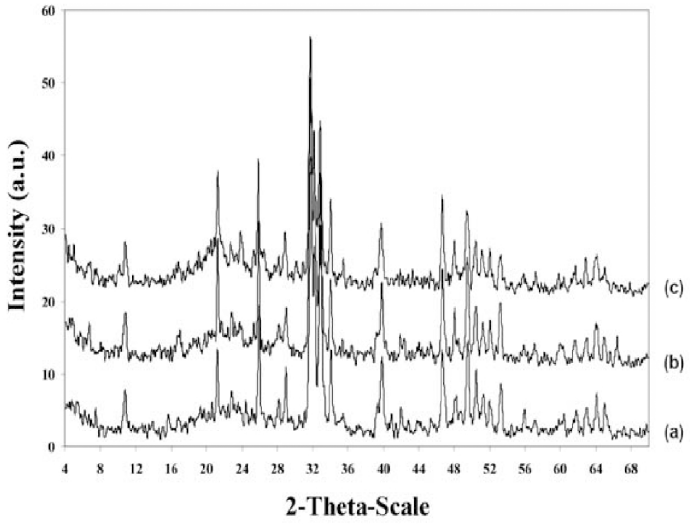

Figure 1. XRD diffraction patterns of the HAp powders obtained at (a): 90 °C; (b): 120 °C; (c): 150 °C.

suspension by centrifuging, washed three times with deionized water to remove the residual CTAB and PEG and then oven-dried at 90 °C for 22 h to yield white powders.

2.3. Characterization

Phase composition of powders was identified by a 3003 PTS Seifert X-ray diffractometer, using Cu-Kα with wavelength 1.5406 A. Fourier transform infrared spectroscopy (FT-IR) studies were carried out by using a Bruker IFS 48. The morphology and particle size of HA powders were investigated by a XL30 Philips SEM.

3. Results and discussion

The XRD patterns of HA samples obtained at 90, 120 and 150 °C are shown in Figure 1. In all samples, all the diffraction peaks could be perfectly indexed to the hexagonal HA with lattice constants of a=9.418 A and c=6.884 A (JCPDS card file no. 09-432). No impurity other than HA is detected by XRD which indicates that the products prepared at different temperatures are monophase of HA. There is also a sign of directional growth in the XRD patterns. In HA standard pattern, intensity of diffracted X-ray relating to (211) plane is assumed to be 100 units and intensity of diffracted X-ray relating to (002) plane will be calculated 40 units. So that the ratio of $I_{(211)}$ to $I_{(002)}$ is equal to 2.5. But when the crystal has preferential orientation in one direction, the intensity of scattered X-ray in plane of that preferred direction will be increased in comparison with intensity of other planes. In HA powders synthesized at 90 °C I211/I002 is equal to 1.92, where for HA powders obtained at 120 and 150 °C is 2.12 and 2.16, respectively, which indicates that directional growth along (002) occurred in all samples and it is more striking in HAppowders synthesized at 90 °C as distinguishable in SEM photographs.

Figure 2 shows the infrared (IR) absorption spectrum of the HA samples obtained at 90, 120 and 150 °C. The FT-IR spectra of all HA samples display the same profile. In all as-prepared powders absorption peaks at 882, 1421 and 1460 cm^{-1} for carbonate ions [11-13] have not been seen. The two peaks at 2852 and 2921 cm^{-1} are attributed to residual CTAB [7], which shows organic surfactant has not been washed away completely and remains in obtained samples. By a simple heat treatment (1 h in 450°C) the residual organic materials will be omitted. The peak at 471.2 cm^{-1} resulted from υ_2 phosphate mode [7, 14, 15] while broad bands at 1633 and 3204 cm^{-1} correspond to adsorbed water

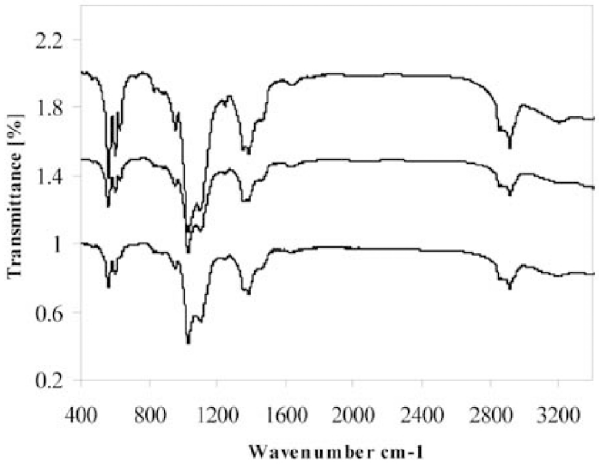

Figure 2. FT-IR spectrum of the HA powders obtained at 90 °C (A; down), 120 °C (B; middel) and 150 °C (C; top).

[7] and lattice H_2O [7], respectively. The characteristic bands for PO_4^{3-} appeared at 565 (PO_4^{3-} bend υ4 [16]), 602.7 (P-O modes [7]), 961 (υ_1 symmetric P-O stretching vibration of the PO_4^{3-} [5, 15]), 1031 (PO_4^{3-} stretching mode [17]) and 1096 cm^{-1}(PO_4^{3-} bend υ_3 [16]). The band at 1382 cm^{-1} is assigned to the N-O stretch of NO_3^-[17]. The broad bands at 3197 and 1655 cm^{-1} correspond to adsorbed water [5, 16]. The two medium sharp peaks at 633 and 3565 cm^{-1} attributed to the O-H bending deformation mode [7] and structural OH [16], respectively, are more distinguishable in HA sample obtained at 150 °C. For powders obtained at 90 °C, they are relatively indistinct which indicates lower crystallinity. So we can conclude that as the hydrothermal temperature increases,

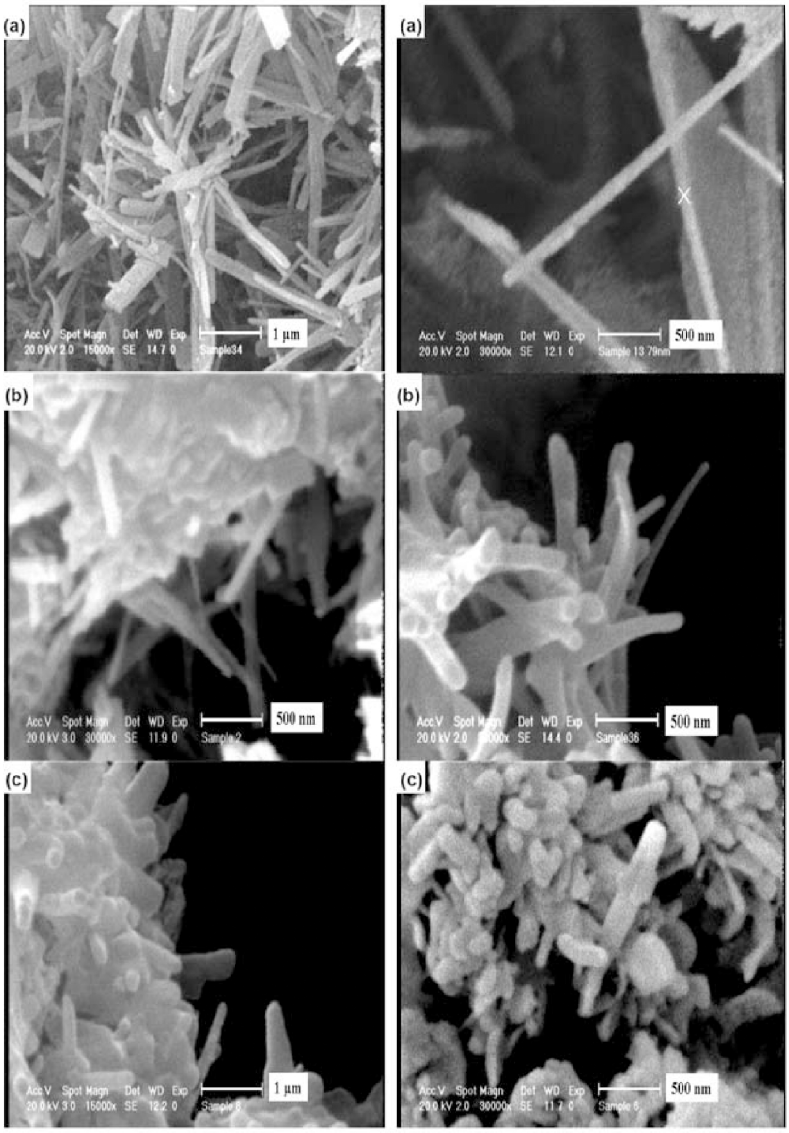

Figure 3. SEM photographs of HA powders obtained at (a): 90 °C; (b): 120 °C; (c): 150 °C.

crystallinity of obtained powders enhances.

Figure 3 illustrates the SEM photographs of HA powders obtained at 90, 120 and 150 °C. As can be seen, all samples have uniform rod-like particles with different aspect ratios and sizes. SEM observations of HA powders synthesized at 90 °C (Figurer 3a) show that the HA crystals are rod-like with straight and flat faces. Also HA particles have a typical diameter of about 40-80 nm and an average aspect ratio of about 16-18. For HA samples obtained at 120 °C (Figure 3b), the long rod-like crystals with mean particle size of about 60-90 nm in diameter and aspect ratio of about 12-15 are observed clearly, but they are aggregated. From the SEM micrographs of HA powders synthesized at 150 °C (Figure 3b), aspect ratio of HA particles is equal to about 4 with the crystal diameter and length of about 80-100 nm and 320-400 nm, respectively. It is also observed that particles have curved and round edges. These results proved that there is not too much difference in the morphology of HA samples obtained at different hydrothermal temperatures, but sizes are heterogeneous. At 90 °C HA particles are much thinner and longer and nano-rods are more distinguishable compared to HA sample obtained at 150 °C. Also they are more uniform size-distributed and separated from each other very well. In all these samples, the mixture of CTAB and PEG has acted as a growth-controlling agent in crystallization of HA.

It has been reported that PEG is a non-ionic surfactant and able to form long chain structures in aqueous solution [7]. Furthermore, in an aqueous system, CTAB would ionize completely and result in a cation with tetrahedral structure. Meanwhile the phosphate anion is also a tetrahedral structure; so CTAB and phosphate ions have charge and structure complementarily with each other [5, 7]. Effect of CTAB in HA crystallization system is thought to be acting as a soft template [5, 7, 18], with the template action resulting in the epitaxial growth of the products [5]. By the charge and stereochemistry complementarily, a process called molecule recognition could be realized at the inorganic/organic interface [19].

It has been proposed that the charge and structure complementarily endow the mixture of CTAB and PEG with the ability to control the crystal growth process [7, 20]. Therefore, HA nano-rods may grow along these long chains and rod-like structure forms when Ca^{2+} ions meet PO_4^{3-} and OH^- ions [7].

4. Conclusion

In summary, HA nano-rods with uniform morphology and controllable size were successfully prepared using CTAB and PEG surfactants under hydrothermal conditions. The products are pure with no carbonated HA. HA powders obtained at different hydrothermal temperatures have rod-like morphology with longitude direction of (002), confirmed by XRD pattern of the samples. At 90 °C HA particles are much thinner, longer and more uniform size-distributed. In addition, the mixture of two surfactants of CTAB and PEG acts as a soft template to regulate the nucleation and crystal growth of HA.

Acknowledgments

The support of Prof. F. Moztarzadeh for supplying of necessary equipment is gratefully acknowledged. The authors would also like to thank Mr. F. Bakhshi for assistance with the FT-IR analysis.

References

[1] Sun Y, Guo G, Wang Z, Guo H. Synthesis of single-crystal HAP nanorods. *Ceram Int* 2006; 32: 951-4.
[2] Hench LL. Bioceramics: From concept to clinic. *J Am Ceram Soc* 1991; 74: 1487-510.
[3] Hench LL. Biomaterials: A forecast for the future. *Biomaterials* 1998; 19: 1419-23.
[4] Rossa R. Hydroxyapatite: Reconstruction of facial

bones. *J Oral Implantol* 1991; 17: 184-92.

[5] Wang Y, Zhang S, Wei K, Zhao N, Chen J, Wang X. Hydrothermal synthesis of hydroxyapatite nanopowders using cationic surfactant as a template. *Mater Lett* 2006; 60: 1484-7.

[6] Mizutani Y, Uchida S, Fujishiro Y, Sato T. Synthesis of monodispersed hydroxyapatite using calcium polyphosphate gels as precursors. *Brit Ceram T* 1998; 97: 105-11.

[7] Liu Y, Hou D, Wang G. A simple wet chemical synthesis and characterization of hydroxyapatite nanorods. *Mater Chem Phys* 2004; 86: 69-73.

[8] Murugan R, Ramakrishna S. Development of nanocomposites for bone grafting. *Compos Sci Technol* 2005; 65: 2385-406.

[9] Kumar R, Prakash KH, Yennie K, Cheang P, Khor KA. Synthesis and characterization of hydroxyl apatite nano-rods/whiskers. *Key Eng Mater* 2005; 284: 59-62.

[10] Yan L, Li Y, Deng Z, Zhuang J, Sun X. Surfactant-assisted hydrothermal synthesis of hydroxyapatite nanorods. *Int J Inorg Mater* 2001; 3: 633-7.

[11] Lee Y, Halm YM, Matsuya S, Nakagawa M, Ishikawa K. Characterization of macroporous carbonate-substituted hydroxyapatite bodies prepared in diffrent phosphate solutions. *J Mater Sci* 2007; 42: 7843-9.

[12] Halcomb DW, Young RA. Thermal decomposition of human tooth enamel and calcify. *Tissue Int* 1980; 31: 189.

[13] Ioku K, Yoshimura M, Munemiya S. Preparation of hydroxyapatite by hydrothermal reaction. *Nippon Kagaku Kaishi* 1985; 1565.

[14] Fowler BO. Structural properties of hydroxyapatite and related compound. *Gaithersburg*, 1968.

[15] Fowler BO. Infrared spectra of apatite. In: Brown WE, Young RA, (editors). *International symposium on structural properties of hydroxyapatite and related compound*. Gaithersburg: MD, 1968.

[16] Panda RN, Hsieh MF, Chung RJ, Chin TS. FTIR, XRD, SEM and solid state NMR investigations of carbonate-containing hydroxyapatite nano-particles synthesized by hydroxide-gel technique. *J Phys Chem Solids* 2003; 64: 193-9.

[17] Anee TK, Ashok M, Palanichamy M, Narayana Kalkura S. A novel technique to synthesize hydroxyapatite at low temperature. *Mater Chem Phys* 2003; 80: 725-30.

[18] Lin K, Chang J, Cheng R, Ruan M. Hydrothermal microemultion synthesis of stochiometric single crystal hydroxyapatite nanorods with mono-dispersion and narrow-size distribution. *Mater lett* 2007; 61: 1683-7.

[19] Shih W, Wang M, Hon M. Morphology and crystallinity of the nanosized hydroxyapatite synthesized by hydrolysis using cetyltrimethylammonium bromide (CTAB) as a surfactant. *J Cryst Growth* 2005; 275: 2339-44.

[20] Sun Y, Guo G, Tao D, Wang Z. Reverse microemultion-directed synthesis of hydroxyapatite nanoparticles under hydrothermal condition. *J Phys Chem Solids* 2007; 68: 373-7.